



Mathematical models application for natural organic matter adsorption onto activated carbon

Abbas H. Sulaymon^a, Abdul-Fattah M. Ali^a, Saadi K. Al-Naseri^{b*}

^a*Environmental Engineering Dept., College of Engineering, University of Baghdad, Iraq*

^b*Ministry of Science and Technology, Baghdad, Iraq*

Tel. +9647901631501; email: Saadikadhum@gmail.com

Received 4 July 2009; accepted 26 May 2010

ABSTRACT

Natural organic matter (NOM) normally exists in raw surface water as a complex mixture of organic compounds, mainly humic acids and fulvic acids. In water treatment plants, free chlorine reacts with NOM and forms a wide range of substances known as disinfection byproducts (DBPs). Granular activated carbon (GAC) adsorption is one of the best available technologies employed for the removal of NOM. Mathematical models for the adsorption of NOM onto GAC in a fixed bed column were reviewed. These models were solved numerically using finite element and orthogonal collocation methods. Of all the tested models, best agreement was obtained between predicted values using homogenous surface diffusion model (HSDM), incorporating adjustment of the average particle size with a proper value of sphericity factor, and experimental results conducted using rapid small scale column tests (RSSCT) for a range of empty bed contact times (EBCT), GAC particle size, and raw water pH. Most of the model parameters were determined experimentally in adsorption equilibrium isotherm and batch reactor experiments.

Keywords: Adsorption; GAC; RSSCT; DOC; NOM; HSDM

1. Introduction

Natural organic matter (NOM) is best described as a complex mixture of organic compounds, mainly humic acids and fulvic acids. Most water sources throughout the world contain NOM. These are always site-specific and even season-specific for the same site. NOM was discovered to react with free chlorine in raw water, forming a wide range of substances known as disinfection byproducts (DBPs) [1]. Two main classes of these compounds are trihalomethanes (THMs) and haloacetic acids (HAAs) which have led to concern by regulators such as the World Health Organization (WHO) and the United States Environmental Protection

Agency (USEPA) following research showing them to cause cancer in laboratory animals [2].

Granular activated carbon (GAC) adsorption is one of the best technologies employed for the removal of NOM. GAC is typically used as a medium in a filter-adsorber or a postfilter-adsorber in many water treatment plants [3]. To predict GAC fixed bed performance, an appreciation of the relevant transport mechanisms is essential in order to incorporate them into an applicable mathematical model.

The objective of this study is to review various relevant mathematical models that describe the dynamics of fixed bed GAC adsorption columns. The models were evaluated by comparing their predictions with experimental results in order to select the most suitable one for NOM removal. The evaluation process of the

*Corresponding author

selected model comprised different operating parameters; namely, empty bed contact times (EBCT), GAC particle sizes, and feed water pH.

2. Mathematical models for GAC adsorption

Fixed bed dynamics are described basically by a set of convection-diffusion equations, coupled with source terms due to adsorption and diffusion inside the adsorbent particles. Solution of these equations gives rise to the prediction of the needed breakthrough curves.

A number of researchers have developed various models to predict one-dimensional transport of adsorbate from the liquid towards the adsorbent particles [4–9]. All of these models have the same following common assumptions:

- Constant convection flow, i.e. plug flow.
- The adsorbate material is non-degradable.
- The column is saturated.
- Pellets of adsorbent are aggregates and considered as spherical particles, uniformly distributed.
- The adsorbent is homogenous.
- Radial concentration gradient is neglected.
- Local adsorption equilibrium exists between the adsorbate adsorbed onto the adsorbent particle surface and the solute in the intra-particle stagnant fluid.

The fixed bed column is usually a cylindrical shape with a pack of GAC (stationary phase). The flow of adsorbate (mobile phase) is vertical along the longitudinal axis of the column. The most general form of the mathematical model incorporates axial dispersion, film mass transfer from the mobile to the stationary phase and both surface and pore diffusion as intra-particle phase mass transport mechanisms [5]. The model is designated as dispersed flow, pore and surface diffusion model (DFPSDM). It consists of two partial differential equations; one for the mobile phase and the other for the stationary phase, as follows:

$$\frac{\partial C}{\partial t} = D_z \frac{\partial^2 C}{\partial z^2} - V_i \frac{\partial C}{\partial z} - \frac{3k_f(1-\varepsilon)}{R\varepsilon} [C - C_p(r=R)], \quad (1)$$

$$\frac{1}{r^2} \frac{\partial}{\partial r} \left[r^2 D_s \rho_a \frac{\partial q}{\partial r} + r^2 D_p \varepsilon_p \frac{\partial C_p}{\partial r} \right] = \frac{\partial}{\partial t} [\rho_a q + \varepsilon_p C_p]. \quad (2)$$

The coupling equation is the adsorption equilibrium isotherm (AEI). The Freundlich adsorption model is perhaps the most widely used mathematical description of adsorption equilibrium in aqueous systems [10]:

$$q = K \cdot C_p^{1/n}. \quad (3)$$

The complexity in solving the nonlinear partial differential equation for stationary phase mass balance (Eq. (2)) gave rise to the assumption of linear equilibrium isotherm relation (i.e., $1/n = 1$) [11]. With this assumption pore and surface diffusion was combined into a single intraparticle diffusion D_i , as follows [5]:

$$D_i = \frac{D_p \varepsilon_p + D_s \rho_a K}{\varepsilon_p + \rho_a K}. \quad (4)$$

Accordingly Eq. (2) is simplified to:

$$\frac{1}{r^2} \frac{\partial}{\partial r} \left[r^2 D_i \frac{\partial C_p}{\partial r} \right] = \frac{\partial C_p}{\partial t}, \quad (5)$$

while Eq. (1) remains unchanged. This model is designated as dispersed flow, combined intraparticle diffusion model (DFCIDM) [5].

Another model that takes into consideration most of the physical transport mechanism as DFPSDM, but ignores pore diffusion and axial dispersion is the homogenous surface diffusion model (HSDM). After neglecting the axial dispersion, the mobile phase equation (Eq. (1)) is simplified to:

$$\frac{\partial C}{\partial t} = -V_i \frac{\partial C}{\partial z} - \frac{3k_f(1-\varepsilon)}{R\varepsilon} [C - C_p(r=R)]. \quad (6)$$

All the previous models were solved numerically because no analytical solution can be applied without further simplification of the models. In order to solve the two partial differential equations of the above-mentioned models the following initial and boundary conditions are utilized:

$$C(z,t) = 0 \quad \text{at} \quad 0 \leq z \leq L, t = 0, \quad (7)$$

$$C(z,t) = C_0 \quad \text{at} \quad z = 0, t > 0, \quad (8)$$

$$\frac{\partial C(z,t)}{\partial t} = 0 \quad \text{at} \quad z = L, t > 0, \quad (9)$$

$$q = 0 \quad \text{at} \quad 0 \leq r \leq R, t = 0, \quad (10)$$

$$\frac{\partial q}{\partial r} = 0 \quad \text{at} \quad r = 0, \quad (11)$$

$$D_s \rho_a \frac{\partial q}{\partial r} = k_f [C(t) - C_p(r=R)] \quad \text{at} \quad r = R. \quad (12)$$

The coupled partial differential equations represent a set of simultaneous, non-linear, partial differential equations that can be solved numerically to provide effluent history (concentration vs. time). They were discretized with respect to space coordinate (Z) using

finite element method and with respect to space coordinate (r) using orthogonal collocation method [12]. The discretization converted the partial differential equations to a set of ordinary differential equations (ODEs). The resulting ODEs were solved using ODE solver provided by MATLAB [13].

Crittenden et al. [5] described another simple model consisting of one partial differential equation. It is designated as dispersed flow local equilibrium model (DFLEM). In this model, the mass transfer resistances are eliminated and the mobile and stationary phases are in equilibrium with each other. Accordingly, the overall simplified column mass balance equation becomes:

$$\left[1 + \frac{(1-\varepsilon)}{\varepsilon} \rho_a K_d\right] \frac{\partial C}{\partial t} = D_z \frac{\partial^2 C}{\partial z^2} - V_i \frac{\partial C}{\partial Z}. \quad (13)$$

The analytical solution for this model is [5]:

$$\frac{C(L, T)}{C_o} = \frac{1}{2} \operatorname{erfc} \left[\frac{Pe^{1/2} (1-T)}{2 T^{1/2}} \right] + \frac{1}{\pi^{1/2}} \left[\frac{T}{Pe} \right]^{1/2} \cdot \frac{(T^2 + 4T - 1) \exp \left[\frac{-Pe(1-T)^2}{4T} \right]}{(T+1)^3}, \quad (14)$$

where T is the throughput and Pe is Peclet Number.

Another model is the linear adsorption model (LAM). It was described and utilized to describe the dynamics of fixed bed column by many researchers [14–18]. The model assumes: linear AEI, pore diffusion controls the intraparticle transport phenomena and the change in the average adsorbent phase concentration \bar{q} is linear. Accordingly, Eq. (2) is simplified to the following form:

$$\frac{\partial \bar{q}}{\partial t} = k_f K (q - \bar{q}). \quad (15)$$

Ramli [19] published a simple analytical solution to this model as follows:

$$\frac{C}{C_o} = \frac{1}{2} \left[1 + \operatorname{erf} \left(\sqrt{\tau} - \sqrt{\xi} + \frac{1}{8\sqrt{\tau}} + \frac{1}{8\sqrt{\xi}} \right) \right], \quad (16)$$

where

$$\tau \approx \frac{k_f K_o Z}{V_i} \left(\frac{1-\varepsilon}{\varepsilon} \right) \text{ and } \xi \approx k_f \left(t - \frac{Z}{V_i} \right)$$

The last model is the logistic function model (LFM). It is based on the use of a mass transfer concept in combination with Freundlich AEI. The model was developed by Clark et al. [20] and used to describe the performance of GAC adsorption systems in drinking

water treatment plants. The model equation can be written as follows [21]:

$$C = \left(\frac{C_o^{n-1}}{1 + A \cdot \exp(-rt)} \right), \quad (17)$$

where r and A are constants in the logistic function. A is defined as:

$$A = \left(\left(\frac{C_o^{n-1}}{C_b} \right) - 1 \right) / \exp(-rt_b), \quad (18)$$

where C_b is the adsorbate concentration after t_b service time, both at breakthrough.

3. Experimental arrangement and procedures

The GAC used in the experiments was a coconut-shell-based variety with an apparent density of 480–490 kg/m³; supplied by Unicarbon, an Italian firm. Four sizes of GAC (0.105, 0.162, 0.230 and 0.353 mm) were obtained by crushing and sieving a sample of GAC (12 × 40 U.S. standard mesh; geometrical mean particle diameter 1.1 mm). The crushed GAC was boiled, washed more than 30 times in distilled water and dried at 105°C for 24 h before being used as an adsorbent. The raw water was taken from Tigris River at Baghdad locality, Iraq. Suspended particles were removed by filtering the water with 5 micron size cartridge filter. Raw water DOC ranged from 1.9 to 2.3 mg/l and its pH was about 7.9

3.1. Rapid small-scale column tests

The RSSCT process was developed for evaluating adsorption of organic matter onto GAC by Crittenden et al. [22]. Extensive description of the method with operating parameters can be found in USEPA literature [23]. In this work RSSCT experiments were performed using 8 mm I.D. glass columns packed with 1.5–9 g of the prepared GAC. The GAC bed was 6–36 mm long (corresponding EBCT of 0.5–3 min for small scale columns). The GAC bed was supported by a 200 mesh stainless-steel screen, a layer of glass beads (250–500 μm), and another 200 mesh stainless-steel screen. Glass wool was placed above the GAC to aid in producing plug flow through the GAC bed. Water samples were slowly pumped from a 300 l plastic tank using a stainless steel piston pump at a flow rate of 6 ml/min. Influent and effluent samples were periodically collected for analysis.

3.2. Batch experiments

These were performed to estimate the diffusion coefficients. This was done by adjusting the predicted

batch concentration curves, obtained from the solution of the batch reactor model, to best-fit the experimental results. A 2-liter flask was filled with 1.75 liter raw water, then 0.7 g of activated carbon was added to the flask followed by agitation. The GAC used in these experiments was the same pulverized one prepared for RSSCT. The quantity of activated carbon was calculated using the following mass balance equation:

$$M = \frac{C_o - C_e}{K \cdot C_e^{1/n}} \cdot V. \quad (19)$$

Samples were taken for analysis at least every 30 min during the first 4 h and one sample per hour after that. Samples of the raw water were analyzed before the experiments were started. A mixing speed of 800 rpm was found appropriate and consequently adopted for all batch experiments. Other researchers used the same speed for particle size range from 12 to 20 standard mesh size while 700 rpm was used for smaller sizes [24].

3.3. Adsorption equilibrium isotherm experiments

AEI experiments were conducted using six 250 ml volume bottles. The GAC used in these experiments was the same pulverized one prepared for RSSCT with a mean particle diameters of 0.105 mm. Amounts of GAC weighing from 0.1 to 1.0 mg were added to the bottles, which were then filled with 200 ml raw water to make the GAC dosage from 0.5 to 5.0 g/l. The bottles were kept shaken continuously for 3 d to keep the activated carbon mixed with the raw water [25]. Liquid phase concentrations in terms of dissolved organic carbon (DOC) were obtained for each sample and the reference sample.

3.4. Analytical instruments and analysis

DOC measurements were conducted to reflect NOM content of the raw water using Dohrmann DC-180 Total Organic Carbon Analyzer (USA). The analysis procedure followed that outlined in Standard Method No. 5310C [26].

4. Results and discussion

4.1. Determination of AEI parameters

Freundlich adsorption equilibrium isotherm model was used and its two parameters, K and $(1/n)$, were determined. The initial water DOC was 2.0 mg/l. It was found that Freundlich isotherm model fit the experimental data reasonably well when using the following values K and $(1/n)$:

$$K = 8.325 (\text{mg/g}) (\text{mg/l})^{-1/n}, \quad 1/n = 1.345.$$

4.2. Liquid film mass transfer coefficient calculation

This parameter was calculated using the following correlation [27]:

$$k_f = 2.4V_s / (Sc^{0.58} Re^{0.66}) [\text{m/s}]. \quad (20)$$

In which the Reynolds (Re) and Schmidt (Sc) numbers were calculated as follows:

$$Re = \frac{V_s d}{\nu \varepsilon} \quad Sc = \frac{\nu}{D_l}. \quad (21)$$

Typically, for a kinematic viscosity (ν) of $1.0 \times 10^{-6} \text{ m}^2/\text{s}$, a superficial velocity (V_s) of 0.002 m/s, a particle size (d) of $0.105 \times 10^{-3} \text{ m}$ and a porosity (ε) of 0.4 the value of Re is 0.53. The value of liquid diffusivity coefficient (D_l) was calculated using the following formula [25]:

$$D_l = 2.74 \times 10^{-9} (MW)^{-1/3} [\text{m}^2/\text{s}], \quad (22)$$

where MW is the molecular mass of adsorbate. NOM substances are heterogeneous in nature and values of molecular mass range from less than 500 Da up to more than 30,000 Da [14,28]. However, the majority of these substances fall within the range of 10,000 to 30,000 Da [28]. To appreciate the range of D_l , a small MW (500 Da) and a large MW (30,000 Da) were used. Accordingly, D_l ranged from 3.45×10^{-10} to $0.88 \times 10^{-10} \text{ m}^2/\text{s}$. It was consequently established that a value of $1.0 \times 10^{-10} \text{ m}^2/\text{s}$ fit the experimental results well [29]. Accordingly, the value of k_f was equal to $3.5 \times 10^{-5} \text{ m/s}$. The determined values are well within the range reported by other researchers [30,31].

4.3. Dispersion coefficient calculation

Dispersion coefficient (D_z) was calculated using the following equation [32]:

$$\frac{D_z}{D_l} = 0.67 + 0.5 \left[\frac{V_s d}{\varepsilon \cdot D_l} \right]^{1.2}. \quad (23)$$

A typical value of D_z for a GAC particle size (d) of 0.105 mm was $1.46 \times 10^{-6} \text{ m}^2/\text{s}$.

4.4. Estimation of surface diffusivity (D_s)

Batch experiments for the adsorption of raw water NOM onto GAC were conducted to estimate the values of D_s . The results are shown in Fig. 1 for each GAC

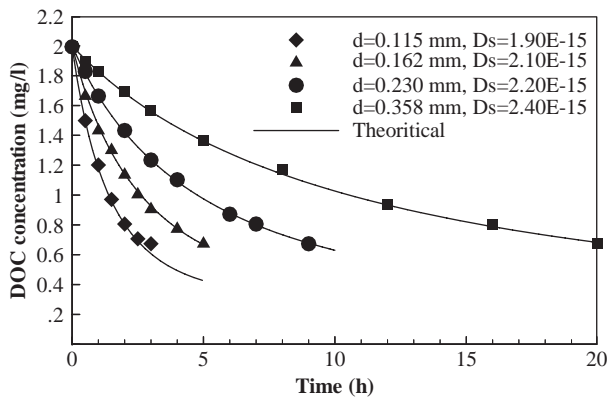


Fig. 1. Batch reactor NOM adsorption onto GAC for various GAC particle sizes.

particle size (0.105, 0.162, 0.230 and 0.353 mm). The determined values for D_s were 1.90, 2.1, 2.2 and $2.4 \times 10^{-15} \text{ m}^2/\text{s}$ for each GAC particle size, respectively. The results showed linear dependence between the surface diffusivity and GAC particle size, being consistent with the assumption made when developing the RSSCT mathematical model [22].

4.5. Estimation of GAC sphericity (ψ)

The necessity of introducing a sphericity shape factor is due to the inadequacy of the particle spherical shape assumption. Its value was found to be significant in predicting the actual GAC column performance. The predictions were found to match the experimental results very well for a sphericity factor value of 0.7. This value was obtained after successive trials to minimize the least square differences between predicted values and experimental results. Other researchers adopted ψ values of 0.69 and 0.62 for GAC of 12×40 and 8×30 standard mesh size, respectively [33].

4.6. Theoretical and experimental breakthrough curves

A comparison was carried out between experimental breakthrough curves obtained from RSSCTs at EBCT of 2.0 min with theoretical breakthrough curves obtained from the various theoretical models. The comparison is illustrated in Fig. 2.

From Fig. 2 it can be concluded that models LFM and LAM gave excellent matching with the experimental results, while models DFLEM and HSDM did not match the experimental results well. Model HSDM applicability was significantly improved by introducing a sphericity factor ψ of 0.7 (designated as HSDM-F in Fig. 2), following the approach of Hutzler et al. [32] which was based on adjustment of the GAC mean particle size. This parameter is most sensitive

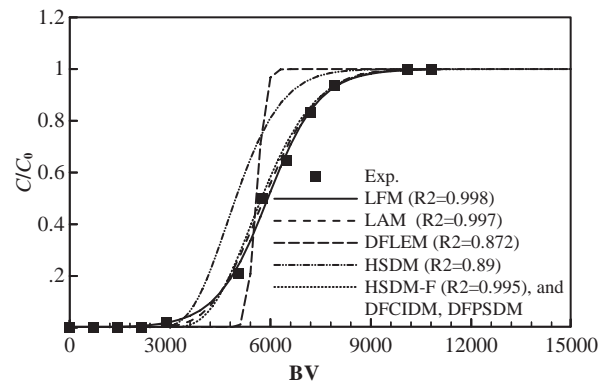


Fig. 2. Comparison between experimental results and predictive models for the case of EBCT = 2.0 min.

to intraparticle mass transport as demonstrated by the sensitivity analysis of the model [22,29].

Models DFPCIDM and DFPSDM were solved using the same numerical algorithm used for HSDM with some modifications. Their results were identical to those obtained by HSDM. This was expected due to the minor effect of pore diffusion because of the tendency of humic substances to be adsorbed on the surface rather than migrating into small pores inside the adsorbent. Accordingly these two models gave no advantage over HSDM.

From the above, it can be concluded that HSDM is the simplest model that incorporates all the effective physical parameters and produces results with acceptable accuracy, provided that the mean particle size is adjusted by the sphericity shape factor. This model was consequently adopted in evaluating the GAC column performance.

4.7. HSDM reliability for various EBCTs, GAC particle sizes and water pH

Comparison of experimental and predicted breakthrough curves are shown in Figs. 3–5. Fig. 3 illustrates breakthrough curves for different EBCTs (0.5, 1.0, 2.0 and 3.0 min; corresponding to large-scale EBCT of 5, 10, 20 and 30 min, respectively). From the figure, it can be seen that breakthrough at $C/C_0 = 0.05$ for the longer EBCT occurs at a larger treated-bed-volumes value than the shorter EBCT. This was expected because as EBCT increases, contact time between the adsorbate and the adsorbent also increases giving the organic matter more opportunity to be adsorbed onto the GAC. However, doubling the EBCT generally does not double the treated water volume. Good agreement exists between experimental results and model prediction.

Fig. 4 shows experimental breakthrough curves at various particle sizes and model prediction. GAC

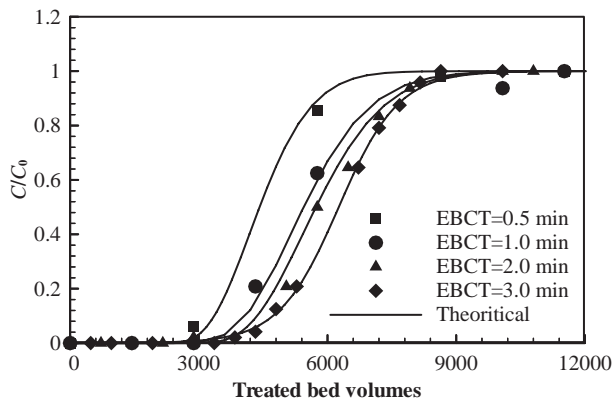


Fig. 3. RSSCT experimental results and predictive fixed bed mathematical model results for different EBCTs.

particle size plays an important role in the amount of NOM adsorbed from raw water. The number of treated-bed-volumes for smaller GAC particle size is higher than that for larger particle sizes. This can be justified as follows: with a smaller particle size, the diffusion pathway from the external surface of the particle to its inside is shorter and the external particle surface area per unit mass of adsorbent is larger – both of which enhance adsorption rate [34]. The predicted values for this case were, also, in close agreement with the experimental results.

In order to test the effect of reducing raw water pH on the nature of the adsorption process, four AEI tests were conducted. The experimental results are shown in Fig. 6. From the figure, it can be concluded that as raw water pH decreases, adsorption capacity (measured in terms of AEI parameter K) increases while the exponent ($1/n$) value decreases. This increase in the adsorption capacity can be explained as follows: NOM is predominately negatively charged; therefore, decreasing the pH renders the negatively charged organic molecules more

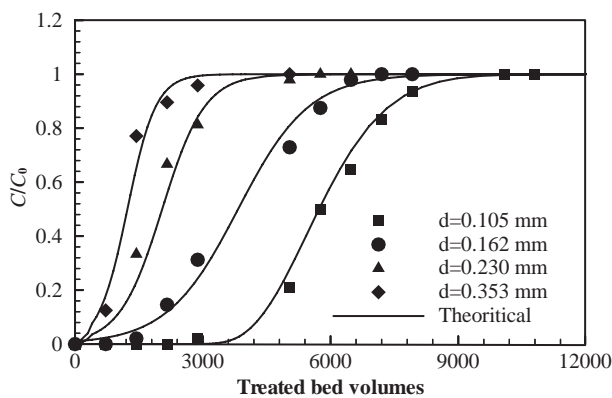


Fig. 4. RSSCT experimental results and predictive fixed bed mathematical model results for different GAC mean particle sizes.

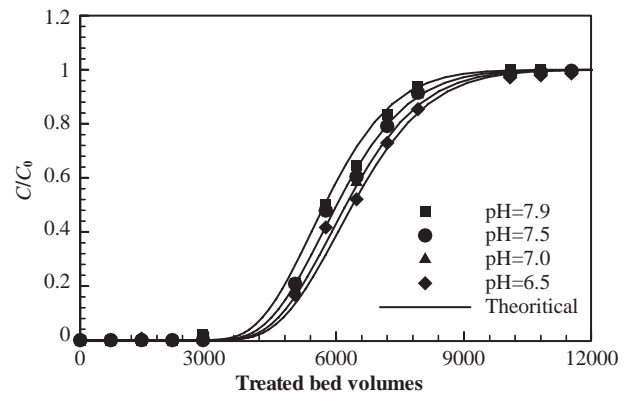


Fig. 5. Effect of raw water pH on the behavior of RSSCT breakthrough curves.

neutral. A neutral molecule is inherently less soluble in water than a charged molecule and, consequently, more adsorbable. The numerical values of K and $(1/n)$ for the various cases are listed in Fig. 6.

Experimental breakthrough results for different raw water pH values along with predicted ones using the obtained values for K and $(1/n)$ are illustrated in Fig. 5. It is clear that the increased adsorption capacity did not reflect a significant effect on the breakthrough behavior. Changing the pH from 7.9 to 6.5 increased K by more than 36%, while it increased the number of treated bed volumes by only 11.5%. Again model curves match experimental results very well.

5. Conclusions

The HSDM is the simplest model that incorporates all the effective physical parameters and produces results with acceptable accuracy. Good agreement was obtained between predicted values by this model and

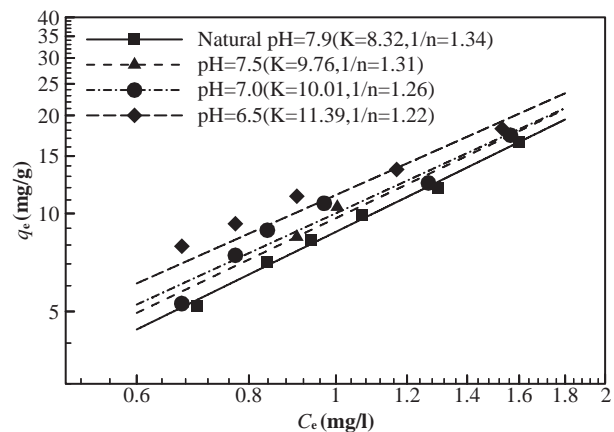


Fig. 6. Effect of raw water pH on the adsorption equilibrium isotherm.

experimental results conducted using RSSCT for a range of EBCT, GAC particle size, and raw water pH; provided that the average GAC particle size is adjusted with a proper value of the sphericity shape factor. Consequently, this model is recommended for predicting NOM adsorption from raw surface water by GAC fixed columns.

Symbol

A	Constant in the logistic function model, –
C	Bulk adsorbate concentration, g/m^3
C_e	Equilibrium adsorbate concentration, g/m^3
C_b	Breakthrough concentration, g/m^3
C_o	Influent concentration, g/m^3
C_p	adsorbate concentration within the pores, g/m^3
d	Geometrical mean diameter of GAC particles, mm
D_i	Intra-particle diffusion coefficient, m^2/s
D_l	liquid diffusivity coefficient, m^2/s
D_p	Pore diffusion coefficient, m^2/s
D_s	Surface diffusion coefficient, m^2/s
D_z	Dispersion coefficient, m^2/s
EBCT	Empty bed contact time, s
K	Freundlich adsorption isotherm capacity constant, $(\text{mg}/\text{g}) (\text{mg}/\text{l})^{-1/n}$
$1/n$	Freundlich adsorption isotherm rate constant, –
K_d	Distribution coefficient, –
k_f	Liquid film mass transfer coefficient, m/s
L	Column length, m
MW	Molecular mass of adsorbate, Da
Pe	Peclet number = $V_i L/D_z$, –
q	Amount of adsorbate adsorbed per unit mass of GAC, mg/g
r	Constant in the logistic function model, –
r	Radial coordinate, m
R	GAC particle radius, m
Re	Reynolds number = $V_s d/\nu\epsilon$,
Sc	Schmidt numbers = ν/D_l –
t_b	Column service time at breakthrough, s
T	Throughput = $V_i t/L$, –
V	Water volume in batch reactor, m^3
V_s	Superficial water velocity, m/s
Z	Axial coordinate, m

Greek letters

ϵ	packed bed porosity, –
ϵ_p	core void fraction of the particle $(1 - \rho_a/\rho_s)$, –
ρ_a	apparent density of GAC, g/m^3

ρ_s	solid particles real density, g/m^3
γ	inematic viscosity, m^2/s
ψ	sphericity, ratio of the surface area of equivalent-volume sphere to actual surface area of particle, –

Mathematical models abbreviations

DFCIDM	dispersed flow, combined intra-particle diffusion model, [equations 1 and 5]
DFLEM	dispersed flow local equilibrium model, [equations 13 and 14]
DFPSDM	dispersed flow pore and surface diffusion model, [equations 1 and 2]
HSDM	homogeneous surface diffusion model, [equations 5 and 6]
HSDM-F	homogeneous surface diffusion model, with sphericity shape factor of 0.7
LAM	linear adsorption model, [equations 15 and 16]
LFM	logistic function model, [equation 17]

References

- [1] J.J. Rook, Formation of haloforms during chlorination of natural waters, *Water Treat. Exam.*, 23 (1974) 234.
- [2] D.A. Fearing, J., Banks, D., Wilson, P.H. Hillis, A.T., Campbell, and S.A. Parsons, NOM control options: the next generation, *Water Sci. Technol.: Water Supply* 4(4) (2004) 139–145.
- [3] K.G. Babi, K.M. Koumenides, A.D. Nikolaou, C.A. Makri, F.K., Tzoumerkasb, and T.D. Lekkas, Pilot study of the removal of THMs, HAAs and DOC from drinking water by GAC adsorption, *Desalination*, 210 (2007) 215–224.
- [4] R.M. Clark, Modeling TOC Removal by GAC: The general logistic function, *AWWA*, 79 (1) (1987) 33–37.
- [5] J.C. Crittenden, J. Hutzler Neil, and D.G. Geyer, Transport of organic compounds with saturated groundwater flow: model development and parameter sensitivity. *Water Res.*, March (1986a) 271–284.
- [6] W. Fritz, W. Merk and E.U. Schlunder, Competitive adsorption of two dissolved organics onto activated carbon-III: Adsorption kinetics in fixed beds, *Chem. Eng. Sci.*, 36 (1981) 743–757.
- [7] A. Rasmuson, Exact solution of a model for diffusion and transient adsorption in particles and longitudinal dispersion in packed beds, *AIChE J.*, 27 (6) (1981) 1032–1035.
- [8] D.W. Hand, J.C. Crittenden and W.E. Thacker, Simplified models for design of fixed-bed adsorption systems, *J. Env. Eng.*, 110 (2) (1984) 440–457.
- [9] J.C. Crittenden and W.J. Weber, Predictive model for design of fixed-bed adsorbers: parameter estimation and development, *J. Env. Eng. Div.*, Apr (1978) 185–197.
- [10] P.H. Chen, C.H. Jeng, and K.M. Chen, Evaluation of granular activated carbon for removal of trace organic compounds in drinking water, *Environ. Int.*, 22 (3) (1996) 343–359.
- [11] N.S. Raghavan, and D.M. Ruthven, Dynamic behaviour of an adiabatic adsorption Column II, *Chem. Eng. Sci.*, 39 (1984) 1201–1212.
- [12] B.A. Finlayson, *Nonlinear analysis in chemical engineering*. McGraw-Hill International Co., New-York, 1980.
- [13] Lazo Cesar, Simulation of liquid chromatography and simulated moving bed (SMB) systems. MSc. thesis, Hamburg Technische University, 1999.

- [14] R.S. Summers and P.V. Roberts, Simulation of DOC removal in activated carbon beds, *J. Env. Eng.*, 110 (1) (1984) 73–92.
- [15] L. Markovski, V. Meshko, V. Noveski and M. Marinkovski, Solid diffusion control of the adsorption of basic dyes onto GAC and natural zeolite in fixed bed columns, *J. Serb. Chem. Soc.*, 66 (7) (2001) 463–475.
- [16] A.P. Vargas, M.B. Hecke, A.P. Scheer, C.H. Marchi and M.R. Maciel, Finite element method applied to a monocomponent liquid adsorption model with non-linear isotherm, Internet – Conference GIMC, 2002.
- [17] M. Hokr and J. Maryska, Numerical solution of two-region advection-dispersion transport and comparison with analytical solution, *Proceeding of Algorithm*, 2002, pp. 1–8.
- [18] D.S. Chaudhary, S. Vigneswaran, H.H. Ngo, S.H. Kim, and H. Moon, Comparison of association theory and Freundlich isotherm for describing GAC adsorption, *J. Env. Eng. Sci.*, 2 (2003) 111–117.
- [19] Wan Ramli Wan Daud, *Proceedings of the 2nd Asian-Oceania Drying Conference, Malaysia*, 2001, ms. 115–122.
- [20] R.M. Clark, J.M. Symons, and J.C. Ireland, Evaluating Field scale GAC systems for drinking water, *J. Env. Eng.*, 112 (4) (1986) 744–757.
- [21] R.M. Clark, and B.K. Boutin, Controlling DBP and microbial contaminants in drinking water, EPA-600/R-01/110, Dec., 2001.
- [22] J.C. Crittenden, J.K. Berrigan, D.W. Hand, and B. Lykins, Design of rapid small-scale adsorption tests for a constant diffusivity, *J.WPCF*, 58 (4) (1986b) 312–319.
- [23] USEPA, ICR manual for bench and pilot scale treatment studies. EPA 814/B-96-003, 1996.
- [24] A.P. Mathews and Inna Zayas, Particle size and shape effects on adsorption rate parameters, *J. Environ. Eng.*, 115 (1) (1989) 41–55.
- [25] D.W. Hand, J.C. Crittenden, and W.E. Thacker, User-oriented batch reactor solutions to the homogenous surface diffusion model, *J. Env. Eng.*, 109 (1) (1983) 82–101.
- [26] APHA, *Standard Methods for the Examination of Water and Wastewater*. 20th. Ed., Washington, 1998.
- [27] J.C. Crittenden, Paul Luft and D.W. Hand, Prediction of fixed-bed adsorber removal of organics in unknown mixtures, *J. Env. Eng.*, 113 (3) (1987) 486–498.
- [28] J.K. Check, Characterization and removal of NOM from raw waters in coastal environments, MSc. Thesis, Georgia Institute of Technology, 2005.
- [29] S.K. Al-Naseri, Natural organic matter removal from samples from Tigris River at Jadiriya in Baghdad, Ph.D. Thesis, University of Baghdad, College of Engineering, Environmental Engineering Department, 2006.
- [30] R.S. Summers, and P.V. Roberts, Rate of humic substance uptake during activated carbon adsorption, *J. Env. Eng.*, 113 (6) (1987) 1333–1349.
- [31] W.J. Weber, Preloading of GAC by natural organic matter in potable water treatment systems: Mechanisms, effects and design considerations, *J. Water Supply: Res. Technol. AQUA*, 53 (7) (2004) 469–482.
- [32] N.J. Hutzler, J.C. Crittenden and J.S. Gierke, Transport of organic compounds with saturated groundwater flow: experimental results, *Water Res.*, March (1986) 285–295.
- [33] Michele Clements and Johannes Haarhoff, Practical experiences with granular activated carbon (GAC) at the Rietvlei Water Treatment Plant, *Water SA* 30 (1) (2004) 89–95.
- [34] Y. Matsui, R. Muraes, T. Sanogawa, N. Aoki, S. Mima, T. Inoue, and T. Matsushita, Micro-ground powdered activated carbon for effective removal of natural organic matter during water treatment, *Water Sci. Tech.: Water Supply*, 4 (4) (2004) 155–163.